Pergamon

Biorheology, Vol. 33, No. 1, pp. 17–44, 1996

0006-355X/96 $15.00 + .00

PII S0006-355X(96)00003-0

THE EFFECT OF AGING AND PRESSURE ON THE SPECIFIC HYDRAULIC CONDUCTIVITY OF THE AORTIC WALL

M. D. WHALE , A. J. GRODZINSKY AND M. JOHNSON

Department of Mechanical Engineering, Massachusetts Institute of Technology, Cambridge, MA 02139, USA

Address for correspondence: Dr. M. Johnson, Room 3-264, M.I.T., 77 Massachusetts Avenue, Cambridge, MA 02139, USA; Tel.: (617) 253-7604; Fax: (617) 258-8559; e-mail: markj@mit.edu

ABSTRACT **We measured the specific hydraulic conductivity (K) of the human and bovine aortic wall, two tissues for which K has not been previously reported in the literature, and examined the effects of aging (human) and development (bovine) on K. As part of the study, we also examined the effects of mounting the tissue in a flat or cylindrical configuration and the effects of perfusion pressure. With aging, in the human, we found a modest increase of K with age in a flat geometry; this trend was not apparent in a limited number of measurements in a cylindrical geometry. No significant dependence of K on developmental stage was found in the bovine aortic wall perfused in either a flat or cylindrical geometry. Our results indicate that aging and developmental changes of the aortic extracellular matrix have minimal effects on its hydrodynamic transport properties as measured. Mounting geometry for the aorta has been a concern reported in the literature since Yamartino *et al.* (1974) reported that K in the rabbit was 10-fold lower when measured in a flat geometry than in a cylindrical geometry. We found mounting geometry to make only a small difference in the calf and the cow, (K_{flat} approximately 2/3 of $K_{cylindrical}$), and in the human, we found K to be somewhat higher in the flat geometry than in the cylindrical geometry. Higher perfusion pressures decreased K of bovine tissue in the flat geometry, but pressure was not found to have a significant effect on K in the cylindrical geometry. An analytical model demonstrated that the anisotropic nature of the aortic wall allows it to be compressible (water-expressing) and yet remain at nearly constant tissue volume as the aorta is pressurized in a cylindrical geometry.**

KEY WORDS: Aorta; anisotropic; strain; permeability; compressible; perfusion

Introduction

Transport of fluid and nutrients through connective tissues is determined, in large part, by the composition of their extracellular matrix (Bert and Pearce, 1984; Levick, 1987). The process of aging results in significant compositional changes in the extracellular matrix of connective tissues (Kohn, 1978; Roberts and Roberts, 1973). Therefore, it might be expected that, with aging, there would be a change in the transport characteristics of the various connective tissues. In this study, we examine the effects of aging and development on the specific hydraulic conductivity of the human and bovine aortic wall, respectively.

By specific hydraulic conductivity, we refer to K in Darcy's law defined as $K = \mu QT/(\Delta P\ A)$ where μ is fluid viscosity, Q the flow rate, T the thickness of the porous medium, ΔP the pressure drop across the porous medium and A the cross-sectional area facing flow (Levick, 1987). We use K" to refer to the hydraulic conductivity of a tissue defined as $K'' = K/(\mu T) = Q/(\Delta P\ A)$. K", also called L_p in the literature, is the parameter that has been usually measured in the past to characterize the aortic wall. However, K" is not a property of the aortic wall microstructure but depends also on the thickness of the tissue and the viscosity of the fluid passing through it. K, on the other hand, is an intrinsic property of a porous medium that is entirely characterized by the microstructure of the material and is independent of the macroscopic dimensions of the tissue. (K would be expected to vary regionally due to the spatial variations in the composition of the extracellular matrix, *e.g.*, Massaro and Glatz, 1979. In the current study, we consider only the average K of the aortic wall and its stress-induced variations.)

In previous studies, K" or K has been determined for the aortic wall of the rabbit (Yamartino *et al.*, 1974; Bratzler 1974; Vargas *et al.*, 1979; Tedgui and Lever, 1984; Baldwin and Wilson, 1993) and the pig (Harrison and Massaro, 1976; Parker and Winlove, 1984) (see Table 1). Two geometries have been used for these perfusions: (i) a flat geometry in which a small piece of tissue is cut out of the aorta and placed into a one-dimensional flow cell, and (ii) a cylindrical geometry using a section of the aorta in a more natural shape. Previous work suggested (Yamartino *et al.*, 1974; Bratzler 1974) that tissue mounting might have a significant effect on K. In this study, we also examine the effects of mounting and perfusion pressure on the specific hydraulic conductivity of the aortic wall.

Materials and Methods

Materials

Bovine (calf, approximately 1–3 weeks of age, and cow, 4–5 years of age) tissues were obtained from a local abattoir (Arena & Sons, Hopkinton, MA, USA) and transported to our laboratory in a saline ice bath. Human tissue was obtained post-mortem from Boston area hospitals, and only samples free from obvious signs of cardiovascular disease were used since the normal aging process was of interest. Bovine perfusions were begun within five to 14 hours of death (within 6 hours of excision) and completed within 24 hours of death of the animal; human perfusions were begun within 24 hours of death (within six hours of excisions) and completed within 36 hours of death.

All chemicals were procured from Sigma Chemical Co. (St. Louis, MO, USA). The perfusion fluid was Dulbecco's phosphate buffered saline with

Table 1

The Hydraulic Conductivity and Specific Hydraulic Conductivity of Aortic Wall from Various Previous Experiments

Study	Species	Tissue Geometry	$K'' = \frac{K}{\mu l}$ $\frac{cm^3}{dynes \cdot sec} \times 10^{11}$	K $cm^2 \times 10^{14}$
Yamartino *et al.* (1974)	rabbit	cylindrical	3.8	0.6
Bratzler (1974)	rabbit	flat	0.31	0.05
Vargas *et al.* (1979)	rabbit	cylindrical	7.7	1.2
Tedgui and Lever (1984)	rabbit	cylindrical	4.0	0.6
Baldwin and Wilson (1993)	rabbit	cylindrical	5.6–7.6	0.8–1.1
Harrison and Massaro (1976)	porcine	flat	0.34	0.7
Parker and Winlove* (1984)	porcine	flat	—	0.3

*Endothelium removed in all experiments except Parker and Winlove. All studies except Parker and Winlove report K"; K was computed from K" assuming a tissue thickness of 150 mm for the rabbit and 2000 mm for the porcine (Truskey *et al.*, 1981).

proteinase inhibitors added: ethylenediaminetetraacetic acid (EDTA; 10 mM) to inhibit metalloproteinases; benzamidine hydrochloride (10 mM) to inhibit trypsin-like activity; N-ethylmaleimide (10 mM) to inhibit sulfhydryl-dependent proteinases and also to prevent disulfide exchange; and phenylmethanesulfonyl fluoride (1 mM) to inhibit serine proteinases. These inhibitors prevent tissue degradation by enzymes normally present in the tissue (Sah *et al.*, 1991). In addition, glucose (1 mg/ml) and antibiotics (50 IU/ml procaine penicillin and 60 mg/ml dihydro-streptomycin sulfate; Fry, 1983) were added and the solution was adjusted to a final pH of 7.2. A few drops of fluorescein were added per liter of perfusion fluid to check for leaks.

Tissue Preparation

A section of aorta between the first and fourth set of intercostal arteries was removed, and surrounding fat and loose connective tissue including the adventitia trimmed away. For experiments in a flat geometry, the aorta was

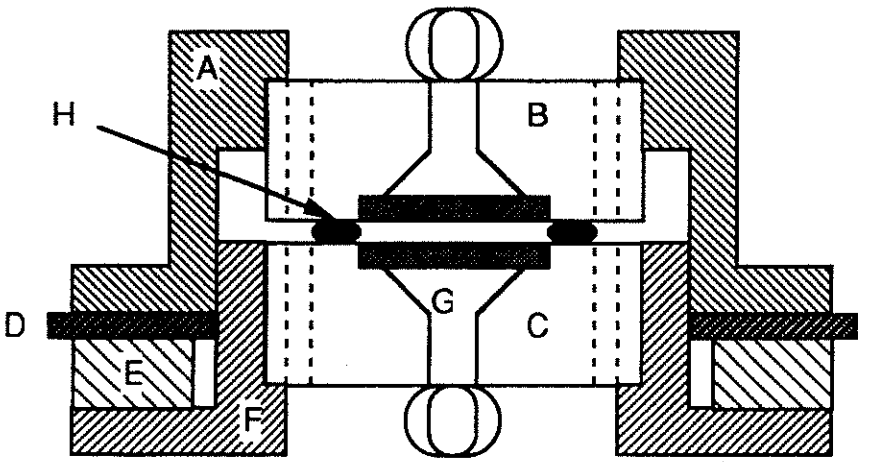

Fig. 1. The schematic representation of the flat flow cell: (A) top flow cell holder; (B) top half of perfusion cell; (C) bottom half of perfusion cell; (D) spacer ring; (E) base spacer ring; (F) bottom flow cell holder; (G) lower porous plate; (H) 'O' ring sealer.

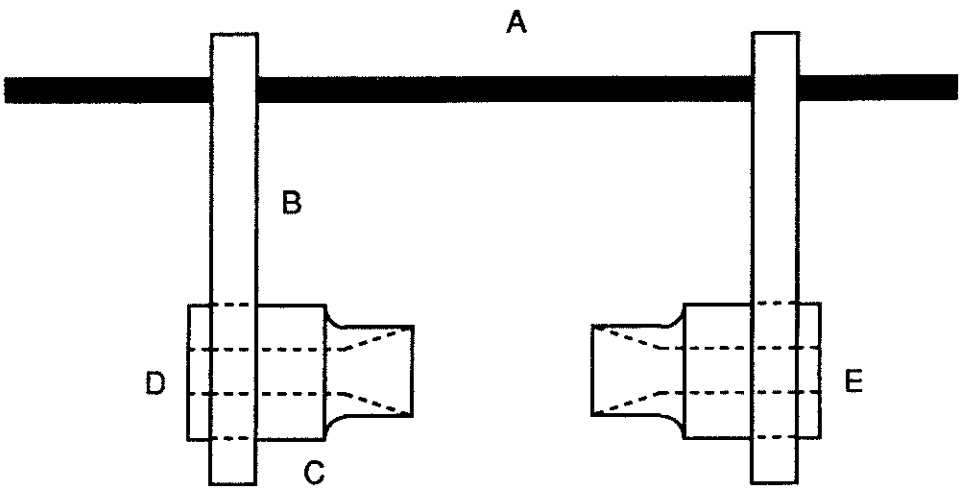

Fig. 2. The schematic representation of the cylindrical mounting technique: (A) the rigid backbone used to set length of specimen; (B) the end brackets for holding the cannulae to the backbone; (C) a cannula; a Plexiglas cylinder to which the aorta is attached on one side and tubing is attached on the other; (D) one end is attached to the syringe pump; (E) one end is attached to the pressure transducer.

split lengthwise between the intercostal arteries, laid flat, and a circular disk of tissue was cut using a 12-mm trephine. As this study concerned the specific hydraulic conductivity of the extracellular matrix of the aorta, the endothelium was removed as Vargas *et al.* (1979) have shown that vessels with an intact endothelium have a flow resistance twice that with the layer removed (Tedgui and Lever, 1984, found a somewhat smaller effect when removing the endothelium; Baldwin and Wilson, 1993, found this effect was pressure-dependent). The endothelium was removed using a moistened cotton-swab. The thickness of the sample was determined using a current-sensing micrometer (Sah *et al.*, 1991). The disk of tissue was placed into the flow cell (Chen, 1991) illustrated in Fig. 1 on the lower porous plate of the flow cell. An 'o' ring was placed on the periphery of the tissue to eliminate radial flow. Based on the measurement of the tissue thickness, a spacer ring was used to set the space between the porous plates to within 20 μm, such that the tissue was compacted five to ten percent of the unpressurized tissue thickness upon sealing in the flow cell (note that at the periphery, the tissue was further compacted by the 'o' ring). The upper perfusion cell was screwed on top with bolts positioned through both the upper and lower perfusion cells that prevent torsional loading as the flow cell holder was tightened.

For experiments conducted with the aorta in the cylindrical configuration, a section was cut between adjacent sets of intercostal arteries since preliminary experiments indicated that ligation of intercostal arteries was insufficient to eliminate flow through the vaso vasorum. The endothelium was stripped from the lumenal surface of the aortic wall by passing a soft sponge soaked with saline through the vessel lumen while continuously rotating the sponge. A similar procedure using a silicone tube was performed by Tedgui and Lever (1984) which had no damaging effects on the intima or media. The effectiveness of the sponging technique was determined in a few specimens (with the kind assistance of Dr. Trinkaus-Randall, Boston University School of Medicine) using light microscopy.

The cylindrical tissue holder (Fig. 2) consisted of a rigid backbone supporting two rectangular brackets. These brackets were free to move along the backbone, and thus, provided a means to adjust the length of the aortic segment being perfused. Into the brackets were placed Plexiglas cannulae machined to various diameters to facilitate the varying sizes of aorta. A small groove in each cannula provided a means to position a thin wire to secure the aortic tissue, and a conical chamber allowed easy removal of bubbles.

The tissue was mounted to the cannulae by securely wrapping a triple loop of stainless steel wire (stainless steel wire, gauge 3, Malin Co., Broock Park, OH, USA) around the aorta while it was placed over the open end of the cannula. By twisting the wire ends and slipping the aorta along the cannula so that the steel loop was in the machined groove, the tissue was secured and completely sealed. Since the aorta shortens upon excision from the body, the brackets were then moved such that the tissue was stretched to 4/3 of its post-excision length (Bergel, 1961; McDonald, 1974; Dobrin, 1978; Vargas *et al.*, 1979; Fry, 1983). The mounted aorta was then set in a small Plexiglas chamber filled with perfusion solution to prevent drying, and the cannulae were connected to the remaining experimental apparatus.

Experimental Device

The device designed to measure the specific hydraulic conductivity must be able to deliver flow rates as low as 10 μl per hour accurately while maintaining constant pressure (to minimize viscoelastic creep) within an aorta containing

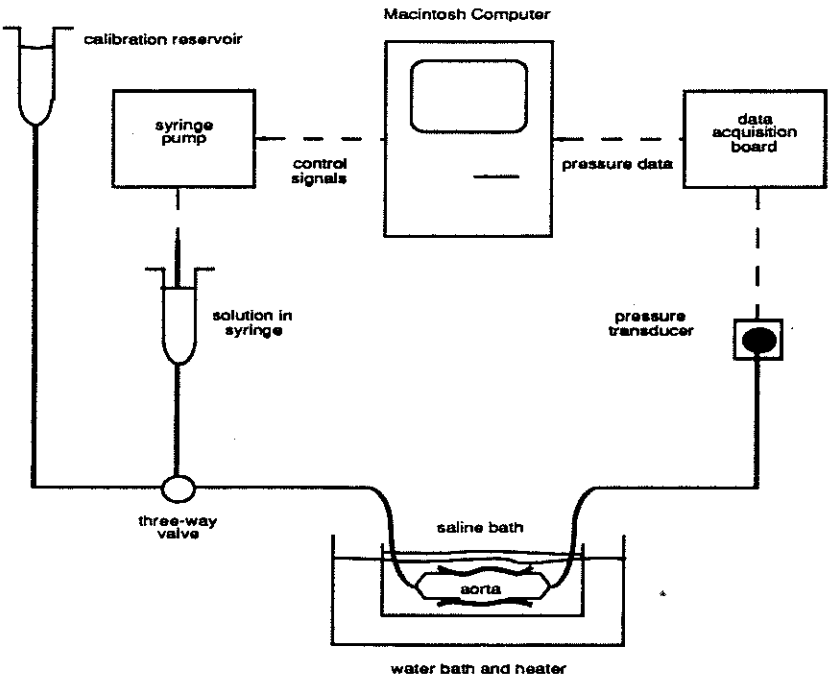

Fig. 3. The schematic representation of the perfusion system with the cylindrical mounting apparatus connected.

(in the cylindrical geometry) several milliliters of fluid. This required an extremely accurate flow source, an external pressurization reservoir, and a sophisticated control scheme.

The final configuration of the apparatus is shown schematically in Fig. 3 for the case of cylindrical samples. The system was set up similarly for the flat specimens. Data acquisition was provided by a Macintosh SE computer with an analog to digital converter board (Lab-SE, 8-bit A/D converter, National Instruments, Austin, TX, USA) used to process the signal from the pressure transducer (Microswitch pressure sensor, 142PC05G, Brownell Co., Woburn, MA, USA). The syringe pump (syringe infusion pump 22, Harvard Apparatus, South Natick, MA, USA) was controlled through the serial port of the computer.

Gas-tight glass syringes (PGC Scientifics, Gaithersburg, MD, USA) of volumes ranging from 100 μl to 500 μl (total volume accurate to within 1% of total syringe volume) were chosen for a particular perfusion depending on the area of aorta being perfused. This syringe was connected via disposable plastic tubing (sterile disposable pressure tubing, 0.050" ID, Mallinckrodt Critical Care, Grand Falls, NY, USA) to all parts of the system. A pressure calibration reservoir, also used for filling the aorta and pressure equilibration was connected to system.

The control scheme is made particularly challenging since the pressure must be very accurately controlled to prevent even minute changes in aortic radius while nonetheless accurately measuring the flow rate entering the tissue and preventing any control scheme instabilities. Thus, the control scheme must both maintain constant pressure and yet also maintain a relatively

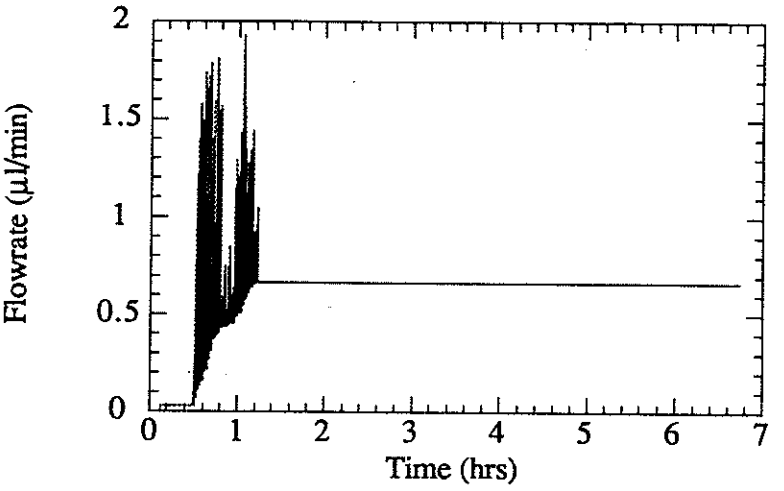

Fig. 4. Typical example of flow rate *vs.* time using the "window" controller (P = 42 mm Hg).

constant flow rate entering the tissue. The control scheme selected to achieve these goals was a hybrid scheme that used a differential control scheme when the pressure varied by more than 0.2 mm Hg from the design pressure, and used an increasingly accurate estimate of the steady-state flow rate to specify a constant flow when the pressure was within this window.

When the pressure was outside the design pressure window, the flow rate was controlled by the following relation:

$$(1) \qquad \frac{dQ}{dt} = 10(P_s - P),$$

where the flow rate (Q) is in units of ml/min, time (t) is in min and the pressure set point (P_s) and system pressure (P) are in units of mm Hg. When the pressure returned within the window, the flow rate was set to the following average value:

$$(2) \qquad Q(t) = \frac{1}{\delta}\int_{t-\delta}^{t} Q(\tau)d\tau,$$

where the averaging time window (δ) was set to 20 minutes. A typical example of the time history of the flow rate is shown in Fig. 4 (the pressure variation during this period was always less than 0.5 mm Hg).

Experimental Protocol

The tissue was maintained at 37° C by placing the mounted aorta in a water bath with a thermostat-controlled immersion heater. All fluid lines were filled with perfusion solution and checked for bubbles, which were removed before pressurization of the lines. The calibration reservoir was set to the desired pressure for the experiment and connected to the mounted specimen. The tissue was subjected to a constant pressure head for approximately one hour to allow the aorta to equilibrate to the new environment. This procedure allowed the aorta to acclimatize, thereby, reducing the effects of creep, and preventing any spontaneous increases in pressure (due to smooth muscle contraction) that would otherwise occasionally occur during the perfusion. During this equilibration period, leakage was checked for by looking for traces of fluorescein (which was added to the perfusion fluid) in the water bath or collection reservoir.

After the initial equilibration period was complete, the data acquisition and control program was started. The pressure to which the specimen was equilibrated was chosen as the pressure set point, and the valve connecting the calibration column was carefully switched to the pump, which gradually took over the supply of perfusion solution to the vessel. This procedure reduced system disturbances when starting the data acquisition. After waiting for the system to reach steady-state (usually one to two hours; Fig. 4), the perfusion was continued for a period of up to six or more hours to determine the specific hydraulic conductivity (Tedgui and Lever, 1984, found that in rabbits the flow rate equilibrated in approximately 30 minutes; Harrison and Massaro, 1976, found in porcine aorta that several hours were required). Regions of steady-state pressure and flow rate were identified as sections where the oscillation in the flow signal is less than 20% of the steady-state value. Only experiments in which such a section lasted for at least four hours were accepted. These sections were integrated to obtain the average values of flow rate, Q, and pressure, ΔP. The equilibrating and perfusing procedure was repeated for each pressure level being investigated on each specimen.

For cylindrical specimens, when the perfusion was complete for each pressure level, the length and outer radius of the aorta were measured using vernier calipers. At the conclusion of the entire perfusion, the unpressurized tissue volume was measured using a displaced volume technique: the aorta was trimmed of the excess length used to mount it and was placed in a water-filled graduated cylinder from which water was removed by use of a pipette to determine the volume displaced. By assuming that the vessel could be approximated as a cylinder, the inner radius, r_i, was determined by using Eq. *(3)*:

$$(3) \qquad \text{vol} = \pi\left(r_e^2 - r_i^2\right)L$$

It should be noted that by using the zero-pressure volume, an assumption of tissue incompressibility has been made. The validity of this assumption is explored below.

The specific hydraulic conductivity was calculated using Darcy's law. In the flat geometry, K was found as:

$$(4) \qquad K = \frac{\mu T Q}{A(\Delta P)},$$

where μ is the viscosity of saline at room temperature, A the cross-sectional area facing flow (0.95 cm^2) and T, the flow-wise length, is determined by the size of the spacer ring, which sets the space between the porous disks, and thus the tissue thickness. In the cylindrical geometry, K was found as:

$$(5) \qquad K = \frac{\mu T Q}{2\pi L \Delta P} \ln(r_e/r_i),$$

where L is the length of the aortic section, r_e its outer radius and r_i its inner radius.

Two preliminary experiments were conducted on porcine tissue to validate the experimental technique in the flat geometry (where previous values were already available in the literature; see Table 1). Experiments were then conducted on 16 calf aortas in a flat geometry with perfusion pressures ranging from 22 to 100 mm Hg (perfusion pressures were chosen below physiological levels to minimize the effects of tissue compression, as we were primarily interested in age and developmental changes of *K* rather than tissue modulus); three of these aortic sections were perfused at two different perfusion pressures. In the cow, 10 perfusions in a flat geometry were performed at pressures from 20 to 88 mm Hg with four of these sections perfused at two different perfusion pressures. In the human, 16 perfusions were conducted in a flat geometry, on tissue from donors ranging in age from 35 to 87 years of age, and at perfusion pressures from 20 to 83 mm Hg, with eight of these sections perfused at two different perfusion pressures.

Using the cylindrical geometry, three preliminary perfusions were conducted on porcine tissue. Experiments were then conducted on 14 calf aortas in a cylindrical geometry at perfusion pressures from 40 to 85 mm Hg, with seven of these sections perfused at two different perfusions pressures; in the cow, eight experiments were conducted in cylindrical geometry at perfusion pressures from 20 to 80 mm Hg with one of these sections perfused at several different pressures; in the human, four experiments were conducted in the cylindrical geometry (ages of 47, 53, 71 and 76) at perfusion pressures of approximately 55 or 75 mm Hg, with two of these tissues perfused at two different perfusion pressures.

A two-sided t-distribution test was used to quantify the statistical significance of differences in measurements of specific hydraulic conductivity with a p-value of 0.05 being the criterion for a statistically significant result. Fits to the data were done using a linear regression. For data sets involving two independent variables (*i.e.*, age and perfusion pressure), a multiple linear regression was done (SYSTAT for the Macintosh, Version 5.2, SYSTAT, Inc., Evanston, IL, USA).

Results

The results of the experiments are summarized in Table 2, which presents the mean specific hydraulic conductivity for each species with the standard error. Considerable variability in K was found in each species, as has been reported by other investigators (Baldwin *et al.*, 1992, 1993).

Studies on Porcine Tissue

The preliminary studies on porcine tissue were done to validate our techniques as data was available from other studies for comparison. Using the flat geometry, we found values of the specific hydraulic conductivity of 1.1×10^{-14}

and 0.82×10^{-14} cm^2, while in the cylindrical geometry, we found values of 0.62×10^{-14}, 0.48×10^{-14} and 0.77×10^{-14} cm^2. Harrison and Massaro (1976) reported a hydraulic conductivity (K") for the porcine, measured in a flat geometry, of 3.4×10^{-12} cm^3/(dyn sec); if we assume a tissue thickness of 2 mm (Truskey *et al.*, 1981), a specific hydraulic conductivity (K) of 0.68×10^{-14} cm^2 is obtained, in good agreement with the values we obtained.

Studies on Bovine Tissue

Experiments were carried out in both flat and cylindrical geometries on both calf and cow aortas, and at variety of perfusion pressures. Figs. 5 and 6 show the experimental measurements of K in a flat geometry for the calf and cow, respectively, as a function of perfusion pressure. While the measurements suggest a decrease in K with increasing perfusion pressure, this relation did not

Table 2

Experimentally Determined Values of Specific Hydraulic Conductivity for Porcine, Bovine and Human Aortic Wall

Species	Cylindrical Geometry Specific Hydraulic Conductivity (K) cm^2	Flat Geometry Specific Hydraulic Conductivity (K) cm^2
Porcine	$(0.62 \pm 0.08) \times 10^{-14}$ n = 3	$(0.95 \pm 0.13) \times 10^{-14}$ n = 2
Bovine (Calf)	$(4.1 \pm 0.7) \times 10^{-14}$ n = 14	$(2.4 \pm 0.3) \times 10^{-14}$ n = 16
Bovine (Cow)	$(3.1 \pm 0.4) \times 10^{-14}$ n = 8	$(2.2 \pm 0.4) \times 10^{-14}$ n = 10
Human	$(1.7 \pm 0.2) \times 10^{-14}$ n = 4	$(2.9 \pm 0.3) \times 10^{-14}$ n = 17

Given as averages with standard error where n is the number of samples tested. If multiple measurements were made on a tissue sample at different pressures, these values were averaged to give one representative value for that sample.

reach statistical significance for either the calf or cow; combining these two data sets (since no statistical difference was found between the calf and the cow: see Table 2), we did find a modest effect of pressure on specific hydraulic conductivity ($dK/dp = -2.5 \pm 1.0 \times 10^{-16}$ cm^2/mm Hg: $p < 0.02$). In the calf (n = 3) and cow (n = 3) aortas that paired measurements were made at two different pressures, the higher pressure was always associated with a lower K.

Figs. 7 and 8 show the results of perfusion of calf and cow aorta, respectively, in a cylindrical geometry; no effect of pressure on specific hydraulic conductivity could be detected. Comparing the results in both a flat and cylindrical geometry between the calf and the cow, no difference could be detected (Table 2).

The difference in values of specific hydraulic conductivity obtained using the two measurement techniques in the bovine did not verify the ten-fold difference between the results of Yamartino *et al.* (1974), and Bratzler (1974). There was, however, a significant difference between the techniques with the flat geometry giving a value of K roughly 2/3 of that measured in a cylindrical geometry ($p < 0.05$).

Studies on Human Tissue

Fig. 9 shows specific hydraulic conductivity (K) of human tissue as a function of pressure, and Fig. 10 as a function of age, both using the flat geometry.

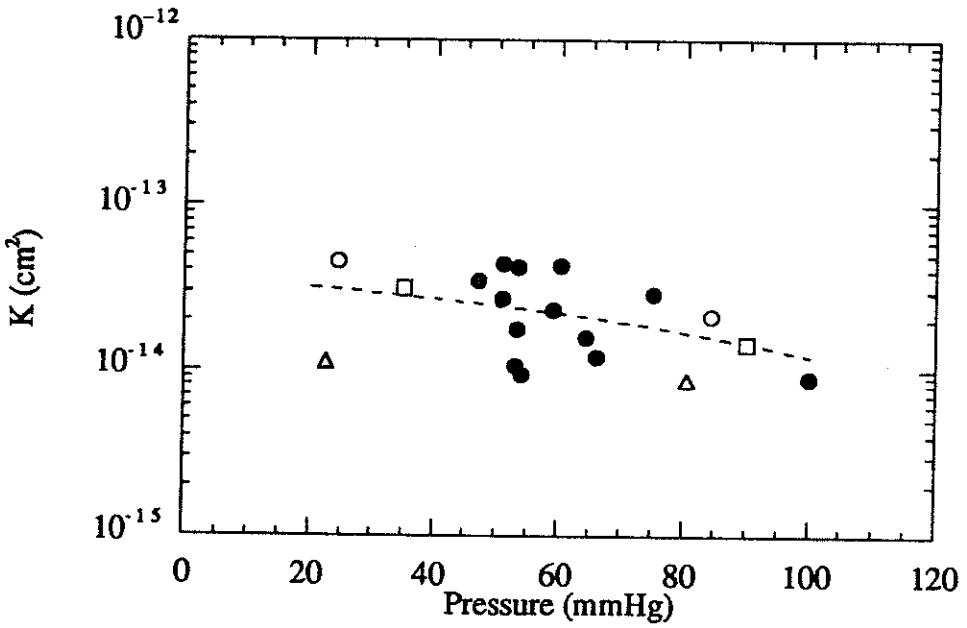

Fig. 5. Specific hydraulic conductivity of the calf aortic wall *vs.* pressure measured in a flat geometry. Closed circles are individual measurements on different tissue samples; each pair of open symbols is a pair of measurements on a single piece of tissue; the line is the best fit to the combined calf and cow data in a flat geometry.

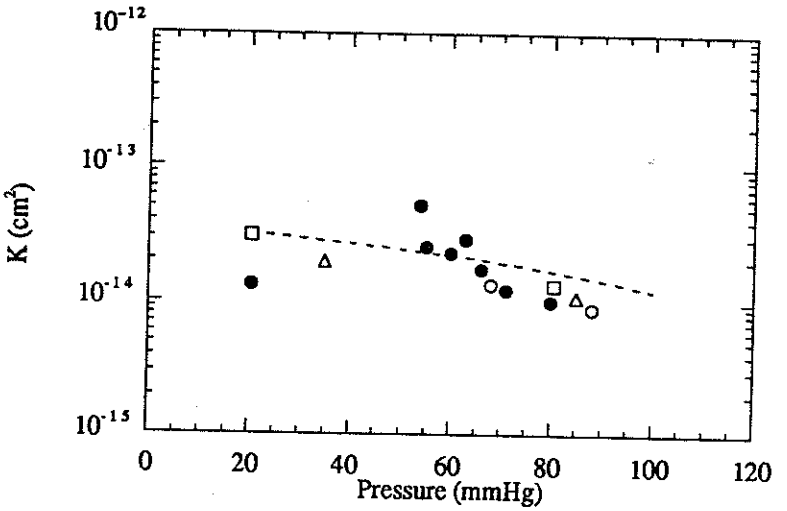

Fig. 6. Specific hydraulic conductivity of the cow aortic wall *vs.* pressure measured in a flat geometry. Closed circles are individual measurements on different tissue samples; each pair of open symbols is a pair of measurements on a single piece of tissue; the line is the best fit to the combined calf and cow data in a flat geometry.

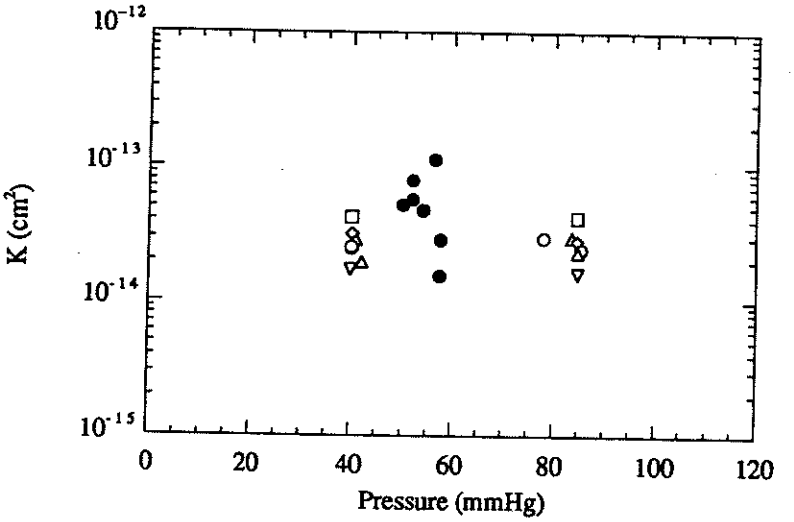

Fig. 7. Specific hydraulic conductivity of the calf aortic wall *vs.* pressure measured in a cylindrical geometry. Closed circles are individual measurements on different tissue samples; each pair of open symbols is a pair of measurements on a single piece of tissue.

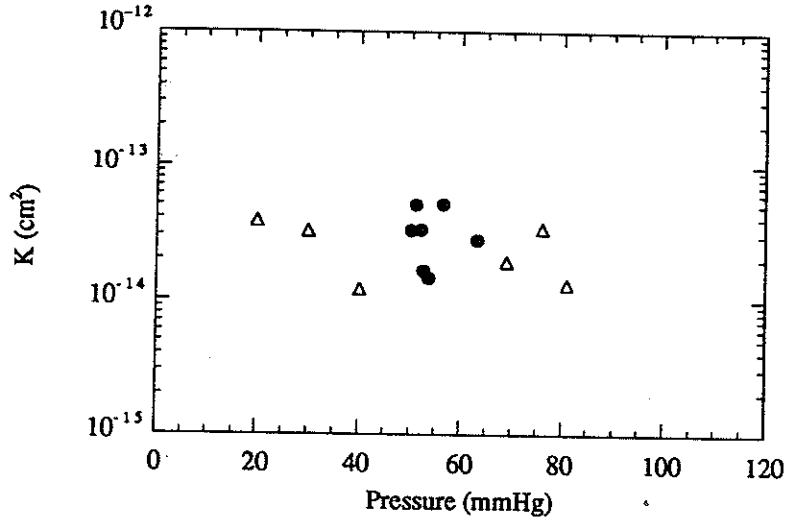

Fig. 8. Specific hydraulic conductivity of the cow aortic wall *vs.* pressure measured in a cylindrical geometry. Closed circles are individual measurements on different tissue samples; open symbols are a series of measurements on a single piece of tissue.

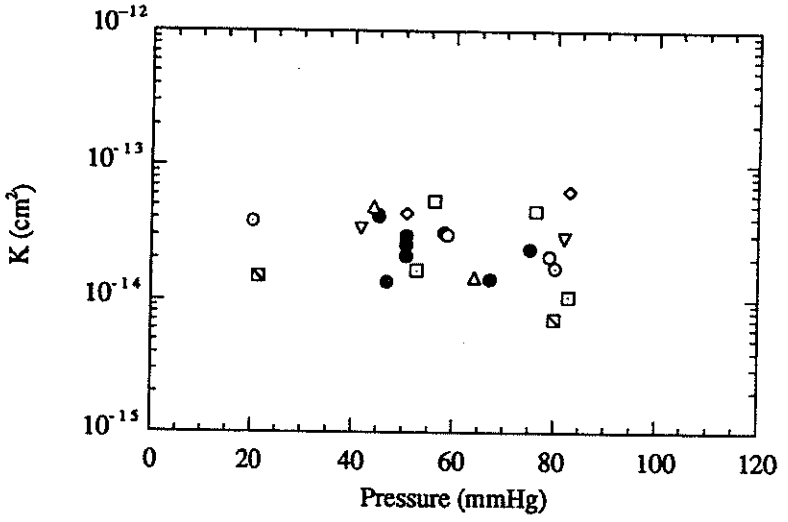

Fig. 9. Specific hydraulic conductivity of the human aortic wall *vs.* pressure measured in a flat geometry. Closed circles are individual measurements on different tissue samples; each pair of open symbols is a pair of measurements on a single piece of tissue.

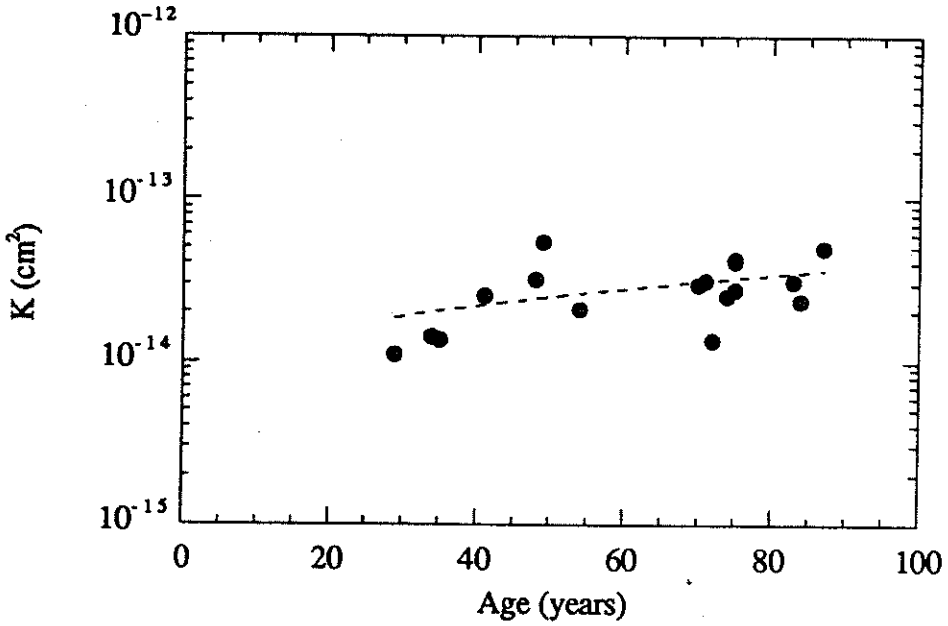

Fig. 10. Specific hydraulic conductivity of the human aortic wall as a function of age measured in a flat geometry. If more than one measurement was made on a tissue sample, the average value was used. Dashed-line is best linear fit to the data.

While seven of the eight aortas in which paired pressure comparisons were made showed a decreased K at higher pressure (as found in the bovine), no statistically significant trend was found. Fig. 10 shows that K of human tissue increases modestly as a function of age in a flat geometry. A multiple linear regression analysis modeling K = a + b*PRESSURE + c*AGE confirmed that there was no statistically significant effect of pressure on K ($p = 0.44$) but there was a statistically significant effect of age ($dK/dAge = 3.1 \pm 1.4 \times 10^{-16}$ cm^2/year: $p < 0.04$)

Table 3 shows the results obtained for K of human tissue in a cylindrical geometry. Only a limited amount of data was available in a cylindrical geometry (it was difficult to procure intact, human aortic samples), and thus conclusions about the effects of pressure and age cannot be drawn although the age-related increase in K found in the flat geometry was not apparent in the cylindrical geometry. Comparison between measurements of human tissue made in a cylindrical geometry with those made in a flat geometry (Table 2) showed a different result than the bovine with the flat geometry having a higher specific hydraulic conductivity than the cylindrical geometry ($p < 0.04$).

Table 3

Individual Experimentally Determined Values of Specific Hydraulic Conductivity for Human Aortic Wall Measured in a Cylindrical Geometry

Age (years)	Pressure (mm Hg)	Specific Hydraulic Conductivity (K) (cm^2)
47	55.5	1.81×10^{-14}
53	57.5	2.56×10^{-14}
53	77.5	1.90×10^{-14}
71	56	1.35×10^{-14}
76	55	1.52×10^{-14}
76	75	1.59×10^{-14}

Theoretical Studies

When the aorta is pressurized in a cylindrical geometry, changes in the internal geometry of the aortic wall are induced by tangential stretching and radial compression. The results from the pressurization studies on cylindrical specimens of calf aorta indicated that increasing pressure had little, if any, effect on K. This result suggested that the volume of the aortic wall is not significantly altered as the pressure is increased (in the range tested), since any net volumetric change would be expected to significantly alter K

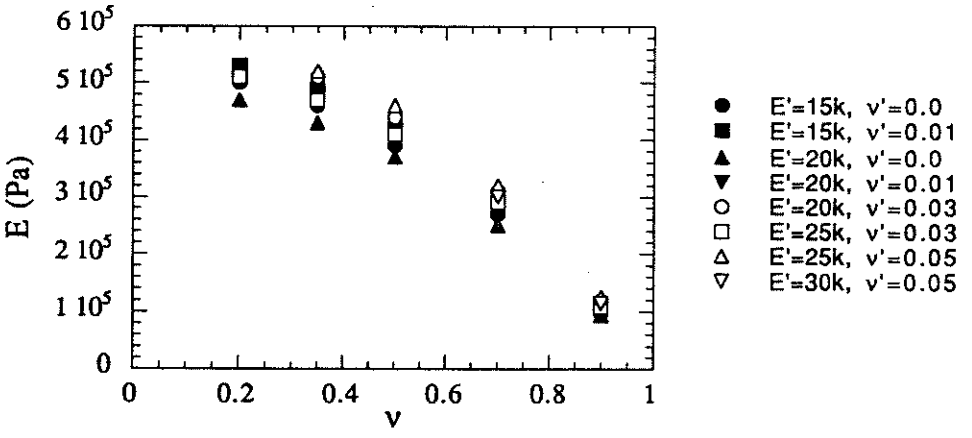

Fig. 11. Model prediction of tangential modulus (E) of calf aorta based on data for radius at varying internal pressure for different assumed values of Poisson's ratio in the tangential plane (ν), radial modulus (E') and Poisson's ratio between the radial and tangential plane (ν').

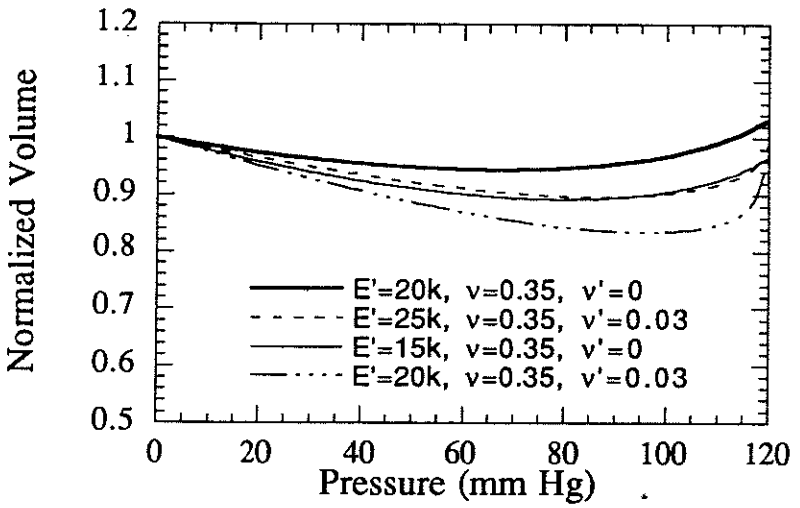

Fig. 12. Model prediction of volume (normalized to unpressurized volume) of calf aorta as a function of pressure for different assumed values of Poisson's ratio in the tangential plane (ν), radial modulus (E') and Poisson's ratio between the radial and tangential plane (ν').

(Klanchar and Tarbell, 1987) (assuming no significant effect of changes in orientation of those extracellular matrix fibers generating flow resistance). However, several investigators have found that the aortic wall is a compressible (water-expressing) tissue (Tickner and Sacks, 1967; Loree *et al.*, 1992), especially at high pressure with the endothelium removed (Tedgui and Lever, 1987). We here employ elasticity theory to investigate the effects of these strains on aortic volume. Our objective is to determine whether the constitutive properties of the aortic wall are consistent with isovolumetric deformations, when pressurized in a cylindrical geometry, while still allowing for the compressibility of this tissue.

The aortic wall can be modeled as a transversely isotropic, compressible material (Tickner and Sachs, 1967), with the circumferential and axial directions having identical moduli (Dobrin, 1986) and the radial direction having a significantly lower modulus (Loree *et al.*, 1992), and with no coupling between the shear stains and the normal stresses (elastic symmetry: Patel *et al.*, 1969) (models of the aorta treating it as a as a biphasic material are described in the Discussion section). The equilibrium mechanical properties of such a material can be completely described by four parameters (for a material not undergoing a torsional loading): E, Young's modulus in the plane of isotropy, E', Young's modulus in the direction perpendicular to the plane of isotropy, ν, Poisson's ratio in the plane of isotropy, and ν', Poisson's ratio in the direction perpendicular to the plane of isotropy. The *Appendix* outlines a model of the aorta as a cylindrical pressure vessel with linear, transversely isotropic material properties. For the purposes of this analysis, the strain-stiffening behavior of the aorta (Nichols and O'Rourke, 1990) was not included in the model, and

thus the moduli determined represent mean values for the given strain distribution. This analysis provides a set of equations that, given a set of material properties, can be solved to obtain the inner radius as a function of internal pressure. This approach was used to calculate the inner and outer radius of the aorta as a function of pressure, and thus the pressure-induced compressibility of the aortic wall was examined.

For use in this model, we estimated the value of radial modulus of the aorta as ranging between 10 kPa (approximately 10% strain) and 30 kPa (approximately 35% strain). This range of values was determined by measuring the compressive radial modulus (Eisenberg and Grodzinsky, 1985) of pieces from two thoracic calf aortas at strains between 0 and 40%; the stress-strain curve showed typical exponential stiffening (Battaglioli and Kamm, 1984) with the first aorta tested varying as $\sigma=850(\exp(7.5\varepsilon)-1)$ and the second as $\sigma=600(\exp(7.75\varepsilon)-1)$ with σ the stress (kPa) and ε the strain. We estimated a value for the tangential Poisson's ratio, ν, of between 0.2 (canine carotid; Dobrin, 1986) and 0.9 (human iliac artery; Tickner and Sacks, 1967), and bounded the value of the radial Poisson's ratio as $\nu' \leq \sqrt{E'/E}$ (Jones, 1975; Loree *et al.*, 1992) (Tickner and Sacks, 1967, found values for this parameter of approximately zero for the human iliac artery held at constant length). Using these values, we determined the value for the tangential elastic modulus, E, that best matched the data for calf outer radius as a function of pressure, constraining the radial modulus to be consistent with the average radial strain.

Measurements of the radius were made on seven calf aortas in the unpressurized state, at a pressure of approximately 40 mm Hg (range: 40–42) and of approximately 84 mm Hg (78-85). In the unpressurized state, the inner radius of the aorta was found to be 0.56 ± 0.03 cm (mean ± S.E.) and the outer radius 0.69 ± 0.03 cm. At 40 mm Hg, the outer radius was 0.71 ± 0.03 cm, while at 84 mm Hg it was 0.79 ± 0.03 cm. The tangential elastic moduli (E) that gave the best fit to this data is shown in Fig. 11 as a function of assumed value for the Poisson's ratio in the tangential plane (ν), radial elastic modulus (E'), and Poisson's ratio between the radial direction and the tangential plane (ν'); only those parameter ranges are shown that are consistent with the parameter constraints. We found that E varied between approximately 100 and 500 kPa, depending largely on the value assumed for ν.

If we used the individual data sets for radius as a function of pressure (instead of the averaged radius from the seven calves as was used to develop Fig. 11), we find that parameter values of E' = 20 kPa, ν' = 0.0 and ν = 0.3 lead to a value of 460 ± 135 kPa for the tangential modulus (mean ± S.D.). Patel (1969) reported that the tangential modulus for the thoracic aorta in the dog was 470 kPa. A similar analysis was done for the single cow aorta that was examined for the effects of pressure on radius. For the same values of E', ν' and ν, we found that E was 2200 kPa, much higher than for the calf ($p < 10^{-4}$).

Our data on hydraulic conductivity suggested that increasing pressure had little if any effect on K in the calf or cow aorta, suggesting that the volume of the aortic wall must not change significantly over the pressure range we examined. Fig. 12 shows how the volume of the calf aortic wall would vary with pressure for various parameter values. Only for very low values of ν' (nearly zero) and values of E' of approximately 20 kPa did the volume of the aortic wall remain relatively constant over the pressure range of interest. However, the pressure-insensitivity of the aorta for these parameters was not dependent on the value of the tangential Poisson's ratio, and thus the estimates for E and ν could not be further refined. The data does show, however, that even though the aortic wall is compressible, the material properties of the vessel wall are consistent with nearly isovolumetric behavior of the wall as pressure is

increased from 0 to 100 mm Hg. We also found (data not shown) that for all cases with an isotropic but compressible aortic wall ($E = E'$, $0 < \nu = \nu' < 0.5$), the aortic wall volume increased as pressure increased.

Discussion

The primary goals of this study were to investigate changes in the specific hydraulic conductivity (K) of human and bovine aortic wall with age and development, respectively. With aging, there are considerable changes that occur in the composition and character of the extracellular matrix of soft connective tissues. There is a general increase in collagen content and the extent to which it is cross-linked (Kohn, 1978; Andreotti *et al.*, 1983). The elastin content increases with age in some connective tissues (Lavker *et al.*, 1987; Kohn 1978; Andreotti *et al.*, 1983) although in the aorta it remains relatively constant (Spina and Garbin 1976; Andreotti *et al.*, 1985). In contrast, the glycosaminoglycan content of most tissues, particularly that of hyaluronic acid, decreases with age (Roberts and Roberts, 1973). While the intervertebral disk shows an approximately 70% loss of glycosaminoglycans due to aging over a lifetime (Hallen, 1958; Urban and McMullin, 1985) and skin (Fleischmajer *et al.*, 1973) and lung (Konno *et al.*, 1982) show a loss of approximately 50%, the loss of glycosaminoglycans in the aorta with age is more modest (approximately 10% between the 4^{th} and 8^{th} decades: Clausen 1962; Stuhlsatz *et al.*, 1982).

Since transport through a tissue is highly dependent on its composition (Bert and Pearce, 1984) and particular its glycosaminoglycan content (Levick, 1987), we have been interested in determining whether K of various connective tissues change with age. In the current study, we have examined the effects of aging and development on K of the aortic wall. As it has been suggested that K of the aorta depends strongly on perfusion geometry (in a single but frequently referenced abstract: Yamartino *et al.*, 1974), and it has been shown that aortic tissue is compressible (Tickner and Sacks, 1967; Loree *et al.*, 1992), a necessary part of this study included examination of the effects of mounting geometry and perfusion pressure on K.

We examined K of porcine, bovine and human aortic wall; previous investigators have examined rabbit and porcine K. Using our data (Table 2) and the data of other investigators (Table 1), we find the porcine aortic wall to have the lowest K ($0.6–1.0 \times 10^{-14}$ cm^2), followed by that of the rabbit ($0.6–1.2 \times 10^{-14}$), the human ($1.7–2.9 \times 10^{-14}$ cm^2) and the bovine ($2.2–4.1 \times 10^{-14}$ cm^2). As these tissue have been shown to have similar concentrations of glycosaminoglycans (Massaro and Glatz, 1979), it is not known what feature of the aortic walls of these different species is responsible for these differences.

The results of our tests performed in a flat geometry show that K of the human aortic wall increases with age at a rate of approximately 2% per year (Fig. 10). In a cylindrical geometry, too few data points were available to establish a trend, but the data did not follow the same age-related trend increase seen in a flat geometry. This suggests that the age-related increase in K found in the flat geometry may relate to strains induced during mounting rather than an intrinsic age-related change in K; this would be consistent with the well-known stiffening of the aortic tissue that occurs with age (Jakatta, 1985).

The availability of bovine aortic samples at two different stages of development provided a means to study the effect of development on the measurement of K. The results of perfusions using calf and cow showed that K is uncorrelated or weakly correlated with development when perfused in either

the flat or cylindrical geometry (Table 2). However, as might be anticipated, there was a significant increase in the stiffness of the tissue with development. Thus, while this tissue significantly increases its elastic modulus during development, it nonetheless maintains its transport characteristics.

In calf and cow aorta measured in a flat geometry, we found that K decreased modestly with increasing pressure (Figs. 5 and 6); in the human, seven out of eight paired experiments in a flat geometry showed K to decrease with increasing pressure, but a statistically significant correlation could not be demonstrated (Fig. 9). As perfusion pressure is increased, the aortic tissue will compress to some extent. While this will decrease the path length for fluid flow (and thereby increase K), the volumetric decrease will increase the concentration of extracellular macromolecules and thereby decrease K. The net result of these two effects is expected to be a modest decrease in K with increasing pressure (Ethier, 1986). The highest pressure we used in this study (100 mm Hg or equivalently 13 kPa) is of the same order as our measurements of the radial modulus of the bovine aortic wall, and thus it would be expected that tissue compression and thereby decreased K would result from increasing pressure, as seen in the bovine specimens. The lack of a statistically significant correlation with pressure in the human samples suggests that the radial modulus of this tissue may be somewhat higher than in the bovine. It should also be noted that in these studies, the tissue was compacted 5 to 10% in the flow cell to prevent leakage; this pre-stress may have minimized the pressure dependency of K.

The results of tests performed in the cylindrical geometry showed no discernible effect of pressure on K in calf or cow tissue (Figs. 7 and 8). Vargas *et al.* (1979) and Tedgui and Lever (1984) found K in the rabbit aorta to be pressure-independent in a cylindrical geometry over a larger pressure range (0–120 mm Hg and 70–180 mm Hg, respectively); Baldwin *et al.* (1992, 1993, 1994) found K'' in the rabbit aorta to be largely pressure-independent between 50 and 150 mm Hg (interestingly, both Tedgui and Lever [1984] and Baldwin *et al.* [1994] found that with the endothelium intact, the hydraulic conductivity of the aortic wall decreased significantly as pressure increased). The lack of correlation of K with pressure for the cylindrical geometry presumably means that the aortic wall volume remains relatively constant as perfusion pressure is increased; Tedgui and Lever (1987) found that between 0 and 70 mm Hg, there was no significant change in hydrated space with increasing pressure. This can be explained by considering the change in cross-sectional shape of the wall as it is pressurized: the circumferential direction will be placed into tension (thereby increasing the tissue volume) while the radial direction becomes compressed (thereby decreasing tissue volume). If the tissue is much stiffer in the circumferential direction than it is in the radial direction (material properties found in the aorta), then these two effects can cancel to a first order approximation. Our analytical model provides support for this finding. We further found that this isovolumetric behavior was a consequence of the anisotropy of the vessel wall since an isotropic, compressible model led invariably to an increasing vessel wall volume (and thus increased K) as the internal pressure was increased.

A reservation should be made regarding the theoretical analysis. We have modeled the aorta as a single phase, compressible material, and as such it should decrease in volume as the hydrostatic pressure acting on the tissue is increased (internal and external pressure on the vessel increased by equal amounts). However, an increase in hydrostatic pressure will not result in fluid motion, and thus the volume of the aorta cannot decrease as the individual constituents of the aorta are incompressible (Carew *et al.*, 1968). In fact, many

biological materials are better characterized as biphasic, incompressible materials (Mow *et al.*, 1984; Barry and Aldis, 1990).

Such biphasic models have been applied to flow through an isotropic aortic wall (Kenyon, 1979; Klanchar and Tarbell, 1987; Kim and Tarbell, 1994). A biphasic, anisotropic model might provide a more accurate characterization of aortic elasticity and transport through the aortic wall, but such a model is beyond the scope of the present work. However, it is useful to examine qualitatively how a single phase, isotropic model would compare to a biphasic, isotropic model. The primary difference between the models lies in the distributed nature of the flow-induced load in the biphasic model that instead appears as a boundary condition in a single phase model. For the flat geometry considered in the current work, this difference leads to a uniform tissue stress in the single phase model equal to the perfusion pressure while in the biphasic model the stress on the solid matrix is zero at the free surface and increases (linearly for a constant K) to the perfusion pressure at the supported surface; tissue compression is, on average, slightly greater in the single phase model. In the case of the cylindrical geometry, the principal difference is a lowering of the radial stress in the biphasic model, with little change in the induced tangential stress that must support both the pressure gradient and the radial tissue stress. The conclusion that the tissue-volume increases as perfusion pressure is increased for a isotropic medium (see *Theoretical Studies* section above) remains unchanged.

Our finding that the aortic wall behaves nearly isovolumetrically as pressure is increased resolves a discrepancy in the literature. The aortic wall is frequently assumed to be incompressible (Patel *et al.*, 1969; Patel *et al.*, 1973; Dobrin, 1978; Vito, 1980; Vito and Hickey, 1980; Chuong and Fung, 1983; Nichols and O'Rourke, 1990) even though all soft connective tissues that have been examined are permeable to water (Levick, 1987) and thus would be expected to express water when they are compressed (Eisenberg and Grodzinsky, 1985). Carew *et al.* (1968) are frequently cited as the basis for the assumption of an incompressible aortic wall. In that study, it was demonstrated that the individual components of the aortic wall are incompressible; however, as noted by the authors, that study could not distinguish water displacement into or out of the aortic wall (a point seemingly missed by many later investigators). However, Dobrin and Rovick (1969) provided experimental results demonstrating that the aortic wall does not change volume as its internal pressure is increased. Our model provides a basis for explaining how the aortic wall can behave isovolumetrically even though it is a compressible tissue. It is tempting to speculate that this isovolumetric behavior may be of some physiological significance: as mean arterial pressure is increased for a period of time (for example, during strenuous exercise; Guyton, 1991), it may be important to keep the volume of the extracellular space relatively constant; otherwise, the concentration of the extracellular moieties (especially GAGs) would be altered, and this might affect cell matrix metabolism (Sah *et al.*, 1989).

Our results suggest that measurements of K in a cylindrical geometry might be less sensitive to perfusion pressure than in the flat geometry. It has been suggested that a further advantage to perfusion in a cylindrical geometry is that K is artificially low when measured in a flat geometry (Yamartino *et al.*, 1974). While we did find a modestly decreased K in a flat geometry as compared to the cylindrical geometry in the bovine (1/3 lower), we did not find the 10-fold difference between flat and cylindrical geometries reported by Yamartino *et al.* (1974). In the human we actually found a somewhat increased K comparing flat geometry to a cylindrical one.

Compared with other tissues, the aorta shows only a small loss of glycosaminoglycans with aging (Clausen, 1962; Stuhlsatz *et al.*, 1982) and the relatively constant value of K with age that we found is consistent with this finding. As in other arterial walls (Fry, 1987), mass transport through the wall of the aorta is dependent on both convection and diffusion (Fry, 1983; Tedgui and Lever, 1985; Kim and Tarbell, 1994). Since the extracellular matrix largely determines both convective and diffusional transport through the arterial wall (Levick, 1987; Bert and Pearce, 1984), changes in K would be expected to be reflected in both transport mechanisms. The relative constant value of K with age suggests that mass transport through the aortic wall does not diminish with age, and that this tissue, like the cornea (Rohen and Lütjen-Drecoll, 1981), experiences less age-related changes than seen in other tissues (the cornea shows no age-related loss in glycosaminoglycans [Buddecke, 1966]). Atherosclerosis and arteriosclerosis, responsible for much of the age-related pathology seen in aortic tissue, likely result from age-related changes to the aortic endothelium (Ross and Glomset, 1976) rather than to intrinsic changes to the body of the aortic wall itself.

Appendix

The aortic wall is modeled as an axially-confined, hollow cylinder (inside radius r_i, outside radius r_e) whose wall is a linear, transversely isotropic material with an anisotropic axis in the radial direction (Tickner and Sacks, 1967; Loree *et al.*, 1992). We consider only a steady-state analysis rather than considering transient consolidation effects (Kenyon, 1979). Following the general scheme of Lehknitskii (1963), the displacements of the inner and outer radii are determined as a function of internal pressure, p, (outside pressure set to zero) and used to calculate the volume. A similar analysis, for an anisotropic cylinder with axial loading and deformation, can be found in Fenn (1957).

A force balance on a differential cylindrical element yields:

$$(A1) \qquad \frac{d\sigma_r}{dr} + \left(\frac{\sigma_r - \sigma_t}{r}\right) = 0.$$

The strain of this differential element in the radial direction is:

$$(A2) \qquad \varepsilon_r = \frac{\left(u + \frac{du}{dr}dr\right) - u}{dr} = \frac{du}{dr},$$

while the strain in the tangential direction can be found as:

$$(A3) \qquad \varepsilon_t = \frac{2\pi(r+u) - 2\pi r}{2\pi r} = \frac{u}{r},$$

where u is the radial displacement of the cylinder. These two strains automatically satisfy the compatibility equation. Note here that we are assuming small strains; larger strains would introduce logarithmic terms.

The generalized Hooke's law relating strains to stresses for a transversely isotropic material is given by Lehknitskii (1963) as:

$$\varepsilon_r = \frac{1}{E'}\sigma_r - \frac{\nu'}{E'}\sigma_t - \frac{\nu'}{E'}\sigma_z$$

$$\text{(A4)} \quad \varepsilon_t = -\frac{\nu'}{E'}\sigma_r + \frac{1}{E}\sigma_t - \frac{\nu}{E}\sigma_z \,,$$

$$\varepsilon_z = -\frac{\nu'}{E'}\sigma_r - \frac{\nu}{E}\sigma_t + \frac{1}{E}\sigma_z$$

where E is Young's modulus in the plane of isotropy, E' is Young's modulus in the direction perpendicular to the plane of isotropy, ν is Poisson's ratio characterizing contraction or expansion in the plane of isotropy in the presence of tension or compression in that same plane, and ν' is Poisson's ratio in the direction perpendicular to the plane of isotropy. The plane of isotropy is the cylindrical surface defined by the z and t directions.

For a thick-walled vessel with axially constrained ends, the deformation is one of plane strain ($\varepsilon_z = 0$), which yields from Eq. *(A4)*:

$$\text{(A5)} \quad \sigma_z = \frac{E}{E'}\nu'\sigma_r + \nu\sigma_t .$$

By introducing this result into the first two equations of Eq. *(A4)* and solving them simultaneously for σ_r and σ_t using Eqs. *(A1)*, *(A2)* and *(A3)* yields the differential equation governing deformation.

$$\text{(A6)} \quad \frac{d^2u}{dr^2} + \frac{1}{r}\frac{du}{dr} - \frac{\beta_{11}}{\beta_{22}}\frac{u}{r} = 0,$$

where the constants are defined as:

$$\text{(A7)} \quad \beta_{11} = \frac{1}{E'}\left(1 - \nu'^2\frac{E}{E'}\right), \quad \beta_{22} = \frac{1}{E}\left(1 - \nu^2\right), \quad \text{and} \quad \beta_{12} = \frac{-\nu'}{E'}\left(1 + \nu\right).$$

The general solution of this differential equation is:

$$\text{(A8)} \quad u = A_1 r^k + A_2 r^{-k} \quad \text{where} \quad k = \sqrt{\frac{\beta_{11}}{\beta_{22}}},$$

where the constants A_1 and A_2 are determined by the boundary conditions:

$$\text{(A9)} \quad \sigma_r(r_i) = -p \quad \text{and} \quad \sigma_r(r_e) = 0.$$

(The minus sign indicates a compressive stress). The constants are found to be:

$$\text{(A10)} \quad A_1 = \left(\sqrt{\beta_{11}\beta_{22}} + \beta_{12}\right)\frac{p r_i^{k+1}}{r_e^{2k} - r_i^{2k}} \quad \text{and} \quad A_2 = \left(\sqrt{\beta_{11}\beta_{22}} - \beta_{12}\right)\frac{p r_i^{k+1} r_e^{2k}}{r_e^{2k} - r_i^{2k}}.$$

Eqs. *(A8)* and *(A10)* can be solved at the inner boundary (r_i) and the outer boundary (r_e), yielding:

$$(A11) \quad r_i - a = p r_i \left[\beta_{22} k \left(\frac{r_e^{2k} + r_i^{2k}}{r_e^{2k} - r_i^{2k}} - \beta_{12} \right) \right]$$

and

$$(A12) \quad r_e - b = \frac{2p\beta_{22} k r_e^k r_i^{k+1}}{r_e^{2k} - r_i^{2k}}.$$

If $k = 1$, Eq. *(A12)* recovers the familiar relationship used to find the modulus of the aortic wall (*e.g.*, Bergel, 1961). Eqs. *(A11)* and *(A12)* can be combined to find:

$$(A13) \quad \frac{r_e}{r_i} \equiv \gamma = (b/a) \left\{ \frac{1 - p\beta_{22} k \dfrac{\left(\gamma^{2k} + 1\right)}{\left(\gamma^{2k} - 1\right)} + p\beta_{12}}{1 - \dfrac{2p\beta_{22} k \gamma^{k-1}}{\gamma^{2k} - 1}} \right\}.$$

For a given pressure, Eq. *(A13)* can be solved iteratively to find γ. Once γ is known, Eq. *(A11)* can be solved for r_i (the equation is now linear in r_i), and thus r_e and the cylinder volume can be determined.

Nomenclature

- a = unpressurized inner radius
- A = cross-sectional area
- b = unpressurized outer radius
- E = elastic modulus in the plane of isotropy
- E' = elastic modulus perpendicular to the plane of isotropy
- k = parameter in displacement equation = $\sqrt{\beta_{11}/\beta_{22}}$
- K = specific hydraulic conductivity, cm^2
- K'' = hydraulic conductivity, $cm^3\ dyne^{-1}\ s^{-1}$
- L = length of cylinder
- p = pressure
- Q = flow rate
- r = radius of cylinder
- T = flow-wise length
- u = radial displacement of cylinder
- ΔP = pressure difference
- μ = viscosity
- β = coefficient in differential equation for displacement
- ε = normal strain
- σ = normal stress

Nomenclature (continued)

ν = Poisson's ratio in plane of isotropy
ν' = Poisson's ratio perpendicular to plane of isotropy

Subscripts

e = external or outer radius
i = internal radius
r = radial direction
t = tangential direction
z = axial direction

References

ANDREOTTI, L., BUSSOTTI, A., CAMMELLI, D., SAMPOGNARO, S., STERRANTINO, G., VARCASIA, G., and ARCANGELI, P. (1985). Aortic connective tissue in ageing—a biochemical study. *Angiology*, December, 872–879.

BALDWIN, A. L., WILSON, L. M. and SIMON, B. (1992). Effect of pressure on aortic hydraulic conductance. *Arterioscler. Thromb. 12*, 163–171.

BALDWIN, A. L. and WILSON, L. M. (1993). Endothelium increases medial hydraulic conductance of aorta, possibly by release of EDRF. *Am. J. Physiol. 264*, H26–H32.

BALDWIN, A. L., WILSON, I. M. and SIMON, B. (1994). Effect of pressure on arterial hydraulic conductance: role of endothelium. In: *Second World Congress of Biomechanics, Amsterdam, The Netherlands*, (abstract). L. Blankevoort and J. G. H. Koolos, Eds., Vol. II, p. 27.

BARRY, S. I. and ALDIS G. K. (1990). Comparison of models for flow induced deformation of soft biological tissue. *J. Biomech. 23*, 647–654.

BATTAGLIOLI, J. L. and KAMM, R. D. (1984). Measurement of the compressive properties of scleral tissue. *Invest. Ophthalmol. Vis. Sci. 25*, 59–65.

BERGEL, D. H. (1961). The static elastic properties of the arterial wall. *J. Physiol. 156*, 445–457.

BERT, J. L. and PEARCE, R. H. (1984). The interstitium and microvacular exchange. In: *The Handbook of Physiology*, Section 2: *The Cardiovascular System*. Volume IV, *Microcirculation*, Part 1. E. M. Renkin and C. C. Michel, Eds.; S. R. Geiger, Exec. Ed., American Physiological Society, Bethesda, MD, USA, Chapter 12.

BRATZLER, R. L. (1974). The Transport Properties of Arterial Tissue. Ph.D. Thesis, Department of Mechanical Engineering, M.I.T.

BUDDECKE, E. and WOLLENSAK, J. (1966). Saure Mucopolysaccharide und Glykoproteine der menschlichen Cornea in Abhängigkeit vom Lebensalter und bei Keratoconus. *Albrecht v. Graefes Arch Klin. Exp. Ophthal. 171*, 105–120.

CAREW, T. E., VAISHNAV, R. N. and PATEL, D. J. (1968). Compressibility of the arterial wall. *Circ. Res. 23*, 61–68.

CHEN, A. Y. (1991). The Hydrodynamic Permeability of Sclera. SB Thesis, Department of Mechanical Engineering, M.I.T.

CHUONG, C. J. and FUNG, Y. C. (1983). Three-dimensional stress distribution in arteries. *J. Biomech. Engr. 105,* 268–273.

CLAUSEN, B. (1962). Influence of age on connective tissue-uronic acid and uronic acid-hydroxyproline ratio in human aorta, myocardium, and skin. *Laboratory Investigation 11,* 1340–1345.

DOBRIN, P. B. and ROVICK, A. A. (1969). Influence of vascular smooth muscle on contractile mechanics and elasticity of arteries. *Am. J. Physiol. 217,* 1644–1651.

DOBRIN, P. B. (1978). Mechanical properties of arteries. *Physiological Reviews 58,* 397–460.

DOBRIN, P. B. (1986). Biaxial anisotropy of dog carotid artery: estimation of circumferential elastic modulus. *J. Biomechanics 19,* 351–358.

EISENBERG, S. R. and GRODZINSKY, A. J. (1985). Swelling of articular cartilage and other connective tissues; electromechanochemical forces. *J. Orthopedic Res. 3,* 148–159.

ETHIER, C. R. (1986). The hydrodynamic resistance of hyaluronic acid: estimates from sedimentation studies. *Biorheology 23,* 99–113.

FENN, W. O. (1957). Changes in length of blood vessels on inflation. In: *Tissue Elasticity.* J. W. Remington, Ed., American Physiological Society, Washington, D. C.

FLEISCHMAJER, R., PERLISH, J. S. and BASHEY, R. I. (1972). Aging of human dermis. *Front. Matrix Biol. 1,* 90–106.

FRY, D. L. (1983). Effect of pressure and stirring on the *in vitro* aortic transmural ^{125}I-albumin transport. *Am. J. Physiol. 245,* H977–H991.

FRY, D. L. (1987). Mass transport, atherogenesis and risk. *Arteriosclerosis 7,* 88–100.

GUYTON, A. C. (1991). *Textbook of Medical Physiology,* W. B. Saunders Co., Philadelphia, PA, USA, p. 198.

HALLEN, A. (1958). Hexosamine and ester sulphate content of the human nucleus pulposus at different ages. *Acta Chem. Scan. 12,* 1869–72.

HARRISON, R. G. and MASSARO, T. A. (1976). Water flux through porcine aortic tissue due to a hydrostatic pressure gradient. *Atherosclerosis 24,* 363–367.

JAKATTA, E. G. (1985). Heart and Circulation. In: *Handbook of the Biology of Aging.* C.E. Finch and E.L. Schneider, Eds., Van Nostrand Reinhold Co., New York, NY.

JONES, R. M. (1975). *Mechanics of Composite Materials.* McGraw-Hill, New York, NY, USA. Equation (2.49).

KENYON, D. E. (1979). A mathematical model of water flux through aortic tissue. *Bull. Math. Biol. 41,* 79–70.

KIM, W.-S. and TARBELL, J. M. (1994). Macromolecular transport through the deformable porous media of an artery wall. *J. Biomedical Engr. 116,* 156–163.

KLANCHAR, M. and TARBELL, J. M. (1987). Modeling water flow through arterial tissue. *Bull. Math. Biol. 49,* 651–669.

KOHN, R. R. (1978). *Principles of Mammalian Aging.* Prentice-Hall Inc., Englewood Cliffs, NJ, USA.

KONNO, K., ARAI, H., MOTOMIYA, M., NAGAI, H., ITO, M., SATO, H. and SATOH, K. (1982). A biochemical study on glycosaminoglycans (mucopolysaccharides) in emphysematous and in aged lungs. *Am. Rev. Respir. Dis. 126,* 797–801.

LAVKER, R. M., ZHENG, P. and DONG, G. (1987). Aged skin: a study by light, transmission electron and scanning electron microscopy. *J Invest. Dermatol. 88,* 44s–51s.

LEVICK, J. R. (1987). Flow through interstitium and other fibrous matrices. *Quarterly J. Exp. Physiol. 72,* 409–438.

LOREE, H. M., KAMM, R. D., STRINGFELLOW, R. G. and LEE, R. T. (1992). Effect of fibrous cap thickness on peak circumferential stress in model atherosclerotic vessels. *Circ. Res. 71,* 850–858.

MASSARO, T. A. and GLATZ, C. E. (1979). Distribution of glycosaminoglycans in consecutive layers of the rabbit aorta. *Artery 5,* 1–13.

McDONALD, D. A. (1974). The elastic properties of the arterial wall. In: *Blood Flow in Arteries,* Williams and Wilkins Co., Baltimore, MD, USA.

MOW, V. C., HOMES, M. H. and LAI, W. M. (1984). Fluid transport and mechanical properties of articular cartilage: a review. *J. Biomechanics 17,* 377–94.

NICHOLS, W. E. and O'ROURKE, M. F. (1990). Properties of the arterial wall. In: *Blood Flow in Arteries,* Lea and Febiger, Philadelphia, PA, USA.

PARKER, K. H. and WINLOVE, C. P. (1984). The macromolecular basis of the hydraulic conductivity of the arterial wall. *Biorheology 21,* 181–196.

PATEL, D. J. and FRY, D. L. (1969). The elastic symmetry of arterial segments in dogs. *Circ. Res. 24,* 1–8.

PATEL, D. J., JANICKI, J. S. and CAREW, T. E. (1969). Static anisotropic elastic properties of aorta in living dogs. *Circ. Res. 25,* 765–779.

PATEL, D. J., JANICKI, J. S., VAISHNAV, R. N., and YOUNG, J. T. (1973). Dynamic anisotropic viscoelastic properties of the aorta in living dogs. *Circ. Res. 32,* 93–107.

ROBERTS, B. and ROBERTS, L. (1973). Aging of connective tissues. *Frontiers of Matrix Biology 1,* 1–45.

ROHEN, J. W. and LÜTJEN-DRECOLL, E. (1981). Ageing- and non-ageing processes within the connective tissues of the anterior segment of the eye. In: *Biochemical and Morphological Aspects of Ageing,* W. E. G. Müller and J. W. Rohen, Eds., Akad. d. Wiss. u. d. Literatur, Mainz-Wiesbaden; Steiner, pp. 157–174.

ROSS, R. and GLOMSET, J. A. (1976). The pathogenesis of atherosclerosis. *N. Engl. J. Med. 295,* 369–420.

SAH, R. L.-Y., KIM, Y.-J., DOONG J.-Y. H., GRODZINSKY, A. J., PLAAS, A. H., and SANDY, J. D. (1989). Biosynthetic response of cartilage explants to dynamic compression. *J. Orthopaed. Res. 7,* 619–636.

SAH, R. L.-Y., DOONG, J.-Y. H., GRODZINSKY, A. J., PLAAS, A. H., and SANDY, J. D. (1991). Effects of compression on the loss of newly synthesized proteoglycan and proteins from cartilage explants. *Arch. Biochem. and Biophys. 286,* 1–10.

SPINA, M. and GARBIN, G. (1976). Age-related chemical changes in human elastins from non-atherosclerotic areas of thoracic aorta. *Atherosclerosis 24,* 267–279.

STUHLSATZ, H. W., LOFFLER, H., MOHANARADHAKRISHAN, V., COSMA, S., and GREILING, H. (1982). Topographic and age-dependent distribution of glycosaminoglycans in human aorta. *J. Clin. Chem. Clin. Biochem. 20,* 713–721.

TEDGUI, A. and LEVER, M. J. (1984). Filtration through damaged and undamaged rabbit thoracic aorta. *Am. J. Physiol 247, (Heart Circ. Physiol. 16),* H784–H791.

TEDGUI, A. and LEVER, M. J. (1985). The interaction of convection and diffusion in the transport of ^{131}I-albumin within the media of the rabbit thoracic aorta. *Circ. Res. 57,* 856–863.

TEDGUI, A. and LEVER, M. J. (1987). Effect of pressure and intimal damage on ^{131}I-albumin and [^{14}C]sucrose spaces in aorta. *Am. J. Physiol. 253, 57, (Heart Circ. Physiol. 22),* H1530–H1539.

TICKNER, E. G. and SACKS, A. H. (1967). A theory for the static elastic behavior of blood vessels. *Biorheology 4,* 151–168.

TRUSKEY, G. A., COLTON, C. K. and SMITH, K. A. (1981). Quantitative analysis of protein transport in the arterial wall. In: *Structure and Function of the Circulation,* Vol. 3. Schwartz, C. J., Werthessen, N. T. and Wolf. S., Eds., Plenum Press, New York, NY, USA.

URBAN, J. P. G. and MCMULLIN, J. F. (1985). Swelling pressure of the intervertebral disc: influence of proteoglycan and collagen content. *Biorheology 22,* 145–57.

VARGAS, C. B., VARGAS, F. F., PRIBYLE, J. G. and BLACKSHEAR, B. L. (1979). Hydraulic conductivity of the endothelial and outer layers of rabbit aorta. *Am. J. Physiol. 236, (Heart Circ. Physiol. 5),* H53–H60.

VITO, R. P. (1980). The mechanical properties of soft tissues—I: A mechanical system for bi-axial testing. *J. Biomechanics 13,* 947–950.

VITO, R. P. and HICKEY, J. (1980). The mechanical properties of soft tissues—II: The elastic response of arterial segments. *J. Biomechanics 13,* 951–957, 1980.

YAMARTINO, E., JR., BRATZLER, R., COLTON, C., SMITH, K., and LEES, R. (1974). Hydraulic permeability of arterial tissue. *Circulation 49, 50,* 273 (Supplement III).

Acknowledgments

Human samples were obtained for this study from autopsies from the Brigham and Women's Hospital, Boston and the Deaconess Hospital, Boston, with the kind assistance of Dr. Richard Lee of the Department of Non-Invasive Cardiology of the Brigham and Women's Hospital. We appreciate assistance from Dr. Vickery Trinkaus-Randall at the Boston University School of Medicine. This work was supported by the National Institute on Aging, R01-AG08289.

Received 5 December 1994; accepted in revised form 28 December 1995.